NUMERICAL SIMULATION OF CRASH-TEST FOR A FORMULA SAE CAR

Simonetta Boria
Giuseppe Forasassi
University of Pisa
Pisa
Paper Number 09-0152

ABSTRACT

Crash-tests and numerical simulations are vital sources of information for designing car safety elements. The aim of this study is the design of a crash-box for a Formula SAE car and the investigation, through a numerical approach, of its dynamic behaviour in frontal impact conditions. The impact attenuator is obtained by the combination of honeycomb sandwich panels and aluminium sheets. Firstly experimental tests and numerical analysis on honeycomb structures were carried out in order to better understand their behaviour and model them properly. Afterwards a global 3D model was built and discretized with finite element method (FEM) in the Ansys code, while the simulation of the crash itself was done by means of the Ls-Dyna code. The crash-box has been optimized regarding several parameters so that the performances required by Formula SAE rules are achieved with minimal structural weight. The obtained results show that the impact attenuator by itself is able to absorb the total kinetic energy with dynamic buckling and plastic deformation of its structure with an average deceleration limited under a 20g value.

INTRODUCTION

The goal of an impact attenuator is to prevent the driver and the car from serious damages in case of impact with an obstacle. In order to meet the requirements of Formula SAE competition, the attenuator must guarantee specific performances in terms of average deceleration values and minimum acceptable dimensions during impact. Moreover the assembly of the crash-box is subjected to the following conditions:

- the impact attenuator must be installed in front of the bulkhead;
- it must be at least 200 mm long (along the main axis of the frame), 200 mm wide and 100 mm high;
- it must not penetrate the front bulkhead in case of impact;
- it must be attached to the front bulkhead by welding or, at least, 4 bolts (M8, grade 8,8);
- it must guarantee safety in case of off-axis and off-centre impact.

A crash-test should be demonstrated by the effectiveness of the energy absorbing structure. In the test the front part of the chassis, including the crash-box and the so called survival cell, is solidly attached to a trolley with a total weight of 300 kg. In this condition the crash-box and the front part of the survival cell hit a rigid barrier at a velocity of 7 m/s. During the test the average deceleration of the trolley must not exceed 20g and the final deformation must be limited to the crash-box only. An impact attenuator can be built with many different materials, like metal alloys and/or reinforced fiber composites. No matter the material, but how it absorbs the impact energy is the most important feature: the attenuator, in fact, must dissipate the total kinetic energy avoiding too high decelerations. An important aspect that can influence the crash-box design is the manufacturing cost. Because of the budget available to the Formula SAE Team, aluminium sandwich structure with hexagonal cells were used in the case discussed in this paper. The advantages of metallic laminas are:

- low cost;
- wide know-how on mechanical behaviour of metals;
- easy design and assembly;

while those of honeycomb core are:

- low weight;
- high energy absorption capability.

This last material is used mainly in aerospace and automotive competitions for obtaining high stiffness-to-weight and strength-to-weight ratios. Honeycomb is designed for being loaded in compression along the cell axis. The cells walls buckle under compression and generate several plastic hinges that absorb energy. Moreover, under bending , honeycomb core separates the skins so that the cross-section holds a high inertia moment. For the application under discussion the geometry and materials characteristics have been chosen and optimized by numerical simulation. Several FE models have been developed, using LS-DYNA code [1], to predict the material structural behaviour under dynamic loads. Actually, crash-tests that certify the quality of the attenuator were not available, but the carried out numerical simulations are considered trustworthy in order to establish the performance of the crash-box in the preliminary design stage.

IMPACT ATTENUATOR: GENERAL SHAPE

Inspired by race competitions, for the attenuator general geometry a truncated pyramidal shape was chosen. With this shape the increasing cross-sectional area prevents from eulerian instability during the deformation. Moreover the angle between the load and the plane of the plates induce bending and the formation of local plastic hinges. With reference to Figure 1, the attenuator can be seen as a blunt hollow beam.

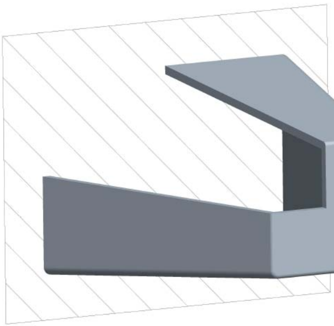

Figure 1. The attenuator as an hollow beam.

This structure is subjected to failure for plastic instability of the sandwich panels (considering the small thickness of the plate, in comparison with the overall dimensions of the body). The plate is substantially a cantilever beam loaded by a complex distribution of forces and moments along its surface. This distribution causes the yielding of a particular section and produces a plastic hinge. With the increase of plasticity deformation in the section, the overall load distribution changes, causing the onset of other plastic hinges. Eventually the main energy absorption mechanism is due almost completely to yielding in the hinges. Along the skins (Figure 2) there is an alternation of hinges and straight zones. The straight pieces are practically not loaded as the hinges are plastically strained.

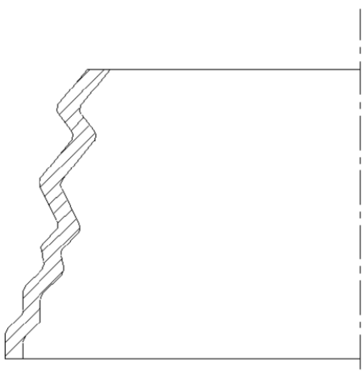

Figure 2. Hinges in plastic buckling.

During loading, the honeycomb skins come in contact one with each other. Now, the honeycomb in the straight piece of the plate is compressed, so it works at best. The hexagonal cells buckle under compression, causing a deep strain into the core; at this time the honeycomb structure stores energy effectively.
In the required performances, the energy to be absorbed is relatively low. Moreover, thanks to previous simulations of crash-boxes made of honeycomb, a well-designed attenuator built with only two sandwich panels seemed to be able to satisfy the quoted requirements..
Inducing the sandwiches fully work in the previously mentioned way, sheets of aluminium assembled between the sandwiches walls demonstrated to be useful to this aim. These membranes create higher stiffness areas and, consequently, trigger the instability and folding of the sandwiches. After the first impact, such aluminium sheets has no structural task; they work only as instability-starter.
A general shape of the attenuator is shown in Figure 3.

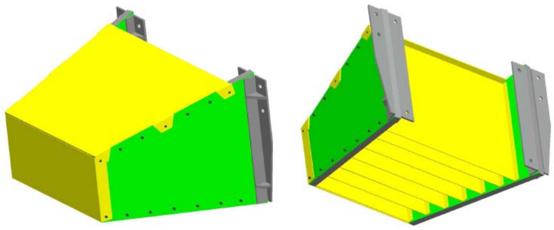

Figure 3. Attenuator's shape.

In the figure a sheet at the top of the attenuator is represented. It avoids that the structure, subjected to a non-frontal impact, behaves as a hinged parallelogram. It is attached directly to the sandwiches and transfers the impact load on both the panels in case of off-axis collision with an obstacle.
The plates are attached to the sandwich panels through rivets. The assembly plan should follow the following steps:

- folding two strips of each plate, for creating the surface to apply the rivets on;
- making holes in sheets and sandwiches for the rivets;
- applying rivets between sheets and panels;
- assembling the attenuator to the front bulkhead via bolts and two ribbed L-shaped joints.

MATERIALS USED

The sandwich panels were made of aluminium AA5052 (Table 1).

Table 1.
Skin alloy properties

	Yield stress (MPa)	Ultimate stress (MPa)	Elongation at break %
AA5052	130	210	9

The other sheets were built with aluminium AA5005 (Table 2).

Table 2.
Aluminium AA5005 properties

Density (kg/m^3)	2700
Elasticity modulus (GPa)	70
Poisson's modulus	0,3
Damping ratio	0,03
σ_y (MPa)	41
σ_u (MPa)	124
ε_{max}	0,07

Compressive tests have been performed on sandwich specimens with quasi-statically deformation. The specimen geometry is described in Table 3, with reference to Figures 4 and 5.
In Figure 6 force-to-specimen area ratio versus displacement-to-initial height ratio behaviours are shown. It is possible to see that an elastic response is followed by a plateau region. After a large displacement, the walls of the cells start touching each other and the core reaches a near total compaction condition. This situation causes a huge increase in stiffness and the core behaves nearly as solid aluminium block. The average stress in the plateau determines the main part of energy absorption capabilities of the honeycomb structure.

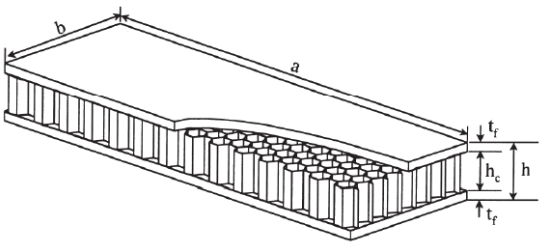

Figure 4. Sandwich panel's geometry.

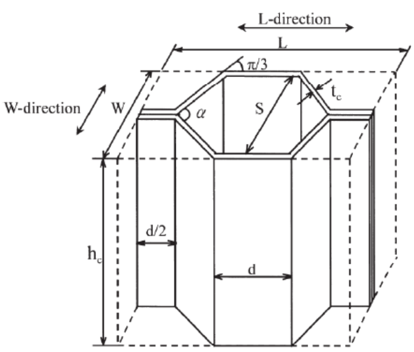

Figure 5. Honeycomb core's geometry.

Table 3.
Dimensions

a (mm)	70
b (mm)	70
h (mm)	13
h_c (mm)	12
t_f (mm)	0,5
S (mm)	6,35
α (°)	120
t_c (mm)	0,0381
d (mm)	3,67

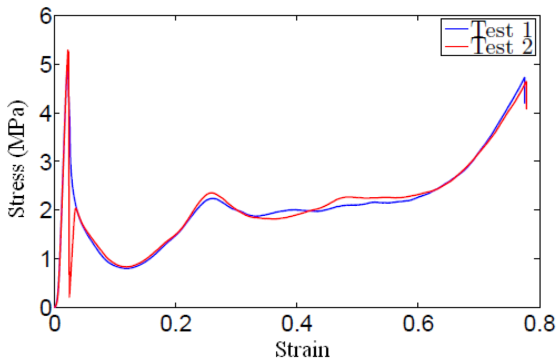

Figure 6. Stress vs strain under compression.

As shown by Enboa Wu and Wu-Shung Yiang [2] crush strength of aluminium AA5052 honeycomb increase linearly with initial impact velocity. There are three possible causes:

- strain rate effects of aluminium;
- compression and temperature increase of air hold into the cells;
- micro-inertial effects.

Aluminium alloys show strain rate effects only at extremely high strain rates (several hundreds per second). Actually, in the considered case, the impact velocity is 7 m/s, so it is hard to achieve high strain rates into a large portion of the sandwiches.
Air within the cells is also negligible, as shown by Hong et al. [3]. Actually air compression alone can not lead to the performance increase experimentally measured.
Inertial effects appear to be the most important factor [4], but their nature is not yet completely understood.
In this study this variation of crush strength is ignored.

MODEL ASSUMPTIONS

Assumptions on materials

The true stress-true strain curve for aluminium alloys can be approximately represented as a bilinear curve (Figure 7). The LS-DYNA code accepts only monotonously increasing material

characteristics curves (so that stress-strain relation is every-where unambiguously defined). Finally the assumed hardening law is isotropic, for computational purpose and the monotonous loading history.
A failure criteria on strains takes into account the final failure of sheets and skins. Failure means a lost of stiffness (e.g. load-carrying capabilities) of broken elements. Failure is detected if elongation at breakage point is reached, in any direction, by an element.
Bulk properties employed for aluminium alloys (kept from literature) are given in Table 2.

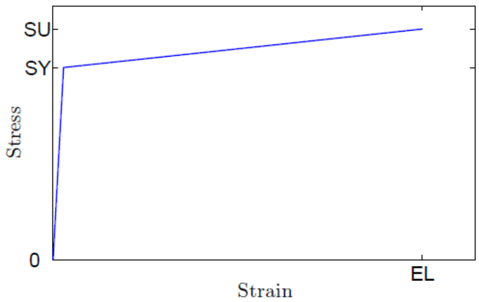

Figure 7. Bilinear curve.

Different approaches for modelling honeycomb structures by FEM exist. They differ in modelling, computational cost and accuracy of the results. Their adoption depends on the specific model size and loading case. A detailed representation of the hexagonal cells can predict the cell wall deformation reasonably well, but it is unsuitable for large-scale models. The model can be simplified by representing the cellular core as an homogenous orthotropic continuum using the honeycomb structure's effective material properties [5].
Three lines describe the true stress-true strain curve of honeycomb before completed compaction. The initial peak point has been neglected, because honeycomb in use was pre-crushed, so it does not show this phenomenon (Figure 8). After compaction honeycomb behaves as solid aluminium, so it shows a linear characteristic with a 70 GPa elasticity modulus. Coordinates of points A, B and C in Figure are shown in the Table 4 below.

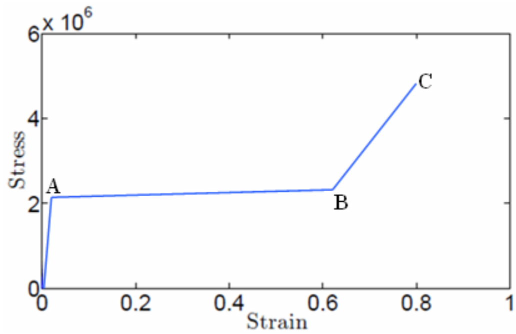

Figure 8. Honeycomb's behaviour

Table 4. Coordinates

	A	B	C
Strain	0,02	0,62	0,833
Stress (MPa)	2,1	2,15	5

The largest mechanical properties are shown in compression along the cell axis. It means that in-plane properties are lower than out-of-plane ones. For obtaining the other orthotropic values some experimental tests were carried out, such as shear, bending and buckling under in-plane compression tests.
An accurate study of the behaviour of honeycomb model present into the software library shows a lack of stiffness in traction along the axis of the cells (Figure 9). Therefore for modelling tensile rigidity link elements have been used, as described in what follows.

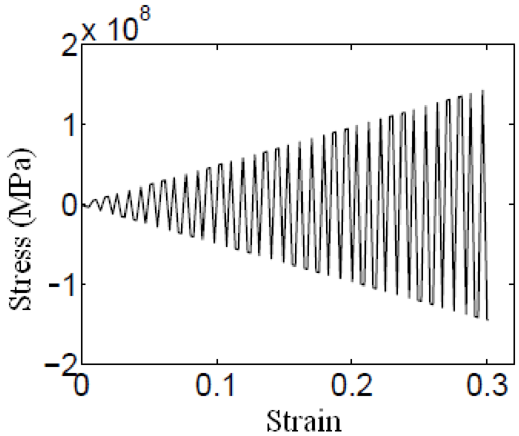

Figure 9. Honeycomb in traction.

Simplification on the model geometry

In order to reduce calculation times, symmetry with respect to two planes has been taken into account. So, only a quarter of the model has been represented (Figure 10). Moreover the upper sheet has been neglected. Actually the constraints imposed on this sheet do not allow the onset of many plastic hinges in bending. So this plate will not really affect energy absorption.
This model does not consider non-symmetric deformation shapes. Symmetry of geometry and load does not allow non-symmetric deformations. As a matter of fact, the manufacturing process will introduce many small shape-defects. However the aluminium sheets can be considered as "big defects" able to induce instability to a much larger extent than small manufacturing defects: this consideration drives to neglect non-symmetric deformations.

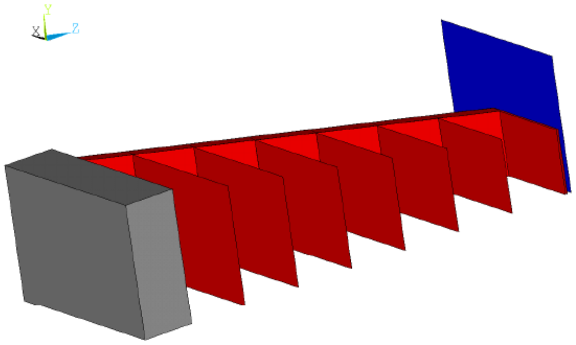

Figure 10. Quarter of model

Constraints have been applied on nodes belonging to the symmetry planes. In particular have been blocked the displacements along the orthogonal direction to the plane and the rotations around the directions in the plane.
Finally a mass of 75 kg represents the vehicle.

Assembly assumptions

The attenuator is hold to the front bulkhead by four ribbed L-shaped joints. Ribbons (Figure 11) and steel bolts attach the joints to the attenuator and to the bulkhead. So, stiffness and non-failure joints conditions during impact are plausible. Therefore the attenuator is considered fully constrained to the vehicle so that some nodes of the sandwich panels (placed near the vehicle) move together with it.

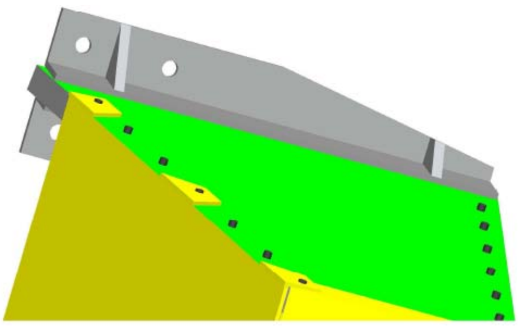

Figure 11. L-shaped joints.

Rivets are not represented in simulation, because of computational cost burden. Moreover failure will reach the aluminium sheets before reaching the rivets. Actually, the load that a sheet and its rivets has to carry is approximately the same and the rivets are much stronger than the sheets. So, sheets are considered attached directly to the corresponding nodes of the skin, without the folded strip mentioned above (Figure 12).

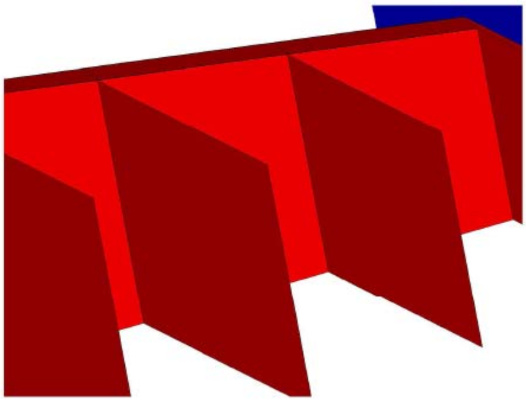

Figure 12. Neglected the folded strips.

Impact assumptions

The crash-box hits actually a rigid wall. The car body is considered rigid too. Assuming rigid wall and body is conservative, because this assumption cancels any time-delay during loading.
During the crash event there are two contacts: aluminium alloy-to-aluminium alloy contact and aluminium alloy-to-wall contact. In literature, friction coefficient between two aluminium surfaces is quoted between 1,1 and 1,7. The coefficient used in simulations is 0,9, because the explicit code does not accept coefficient greater than 1. The same coefficient is used for aluminium-to-wall contact. The heat developed by the hit certainly increases the friction between wall and the aluminium surface and the material of the wall is not a priori known, even if it might be steel.

Elements used

<u>**Shell**</u>
Aluminium sheets, the wall and the skins are meshed with the explicit dynamic element SHELL163. This is a 4-nodes element with both bending and membrane capabilities. It implements a fully-integrated Belytschko-Tsay element formulation, with 5 integration points in the thickness. The quadrature rule for integration is the Gauss one, faster than the trapezoidal rule and accurate enough for this study. Sheets are really thin (1 mm) and the use of a brick element is not justified.

<u>**Brick**</u>
The used explicit brick elements are SOLID164 and SOLID168. The first is an 8-node brick element, while the second is a 10-node tetrahedron one. SOLID168 is more accurate but computationally onerous. Actually, SOLID164 is sufficient for the aim of simulation and moreover has been used fully integrated to avoid the birth of hourglass phenomena.

<u>**Link**</u>
LINK167 is an explicit tension-only spare. It behaves like a cable, with no compressive nor

bending stiffness. This element gives honeycomb tensile rigidity linking the facing nodes of the skins. It is modelled as a spring, for computational saving. Moreover it is not useful to represent stretched honeycomb. The failure of glue between the inner honeycomb nucleus and the outer skins is reached before honeycomb yielding in traction. It is necessary that links reproduce the right tensile stiffness of the honeycomb core. For this aim, honeycomb is considered as a collection of aluminium hexagonal prisms. Each prism is considered as a beam whose area is the area of the transverse section of the cell. The elasticity modulus of aluminium of this beam is 70 GPa. In the model there are so many links as nodes on a skin. An equivalent area must be assigned to the link, so that the total stiffness of links equals the total stiffness of prisms.
The equivalent area is:

$$A_{eq} = \frac{A_{HEX} N_{HEX}}{N_N} \qquad (1).$$

where
- A_{eq} is the equivalent area to be assigned to the link (m^2);
- N_{HEX} is the number of hexagonal prisms filling the area of the skin;
- N_N is the number of nodes filling the area of the skin;
- A_{HEX} is the area of the transverse section of the prism (m^2).
In particular

$$A_{HEX} = \frac{4St_c}{\sqrt{3}} \qquad N_{HEX} \approx \frac{A_S}{(S^2\sqrt{3})/2} \qquad (2).$$

where
- A_S is the skin surface area (m^2).
Stiffness equivalency is obtained with good accuracy.
A failure criteria is given for the links too. Links break when the tensile stress reaches the ultimate stress of glue (in literature 15,5 MPa). So also the glue is simulated.

SUMMARY OF THE RESULTS

The length of the attenuator and the number of trigging sheets have been changed in each simulation. The number of sheets goes from 4 to 7 (no more than 7 sheets were assumed for technological reasons) and the lengths simulated are 300, 350 and 400 mm (no longer than 400 mm for weight saving). Under 300 mm the acceleration shows very high peaks. Actually, safety purposes induce to try to reduce the maximum acceleration values as much as possible.

The displacement during impact has to be checked because it is an index of the safety margin. A well carried out simulation shows the behaviour of the model, but the real attenuator is a bit different (for technological reasons) from the numerical model. This aspect is considered by the displacement-to-initial length ratio. This ratio must be far enough from 1, so that the attenuator can tolerate technological differences from the numerical model.
In Figures 13, 14 and 15 are shown the accelerations resulting from simulations of the attenuator. Accelerations are divided by 20g, for improving the readability of the plot.

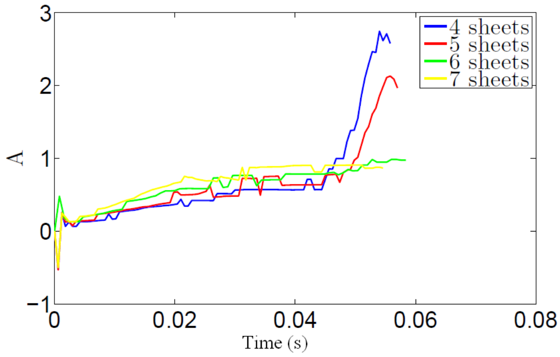

Figure 13. Acceleration vs time (300 mm long).

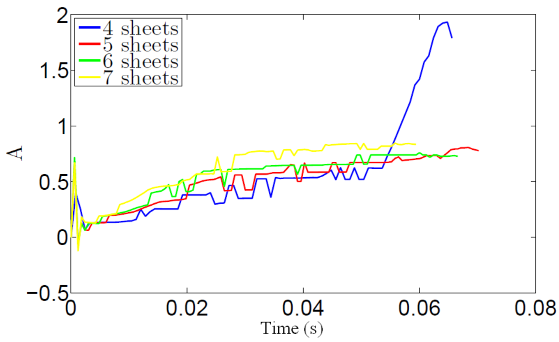

Figure 14. Acceleration vs time (350 mm long).

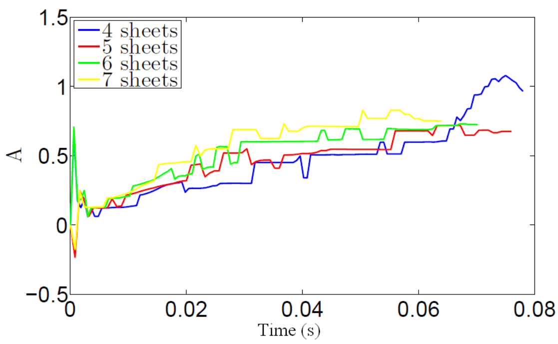

Figure 15. Acceleration vs time (400 mm long).

A 300 mm long attenuator with 4 or 5 transverse plates shows high peaks in the acceleration plot. The same phenomenon is shown by the 350 mm long attenuator with 4 sheets. This behaviour corresponds to a high final compression level reached (more than 80% of initial length) by the attenuator, as shown in Figures 16, 17 and 18. This plots show the compression versus time of the attenuator divided by the initial length.

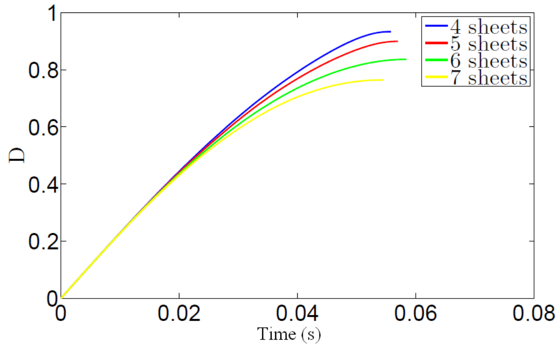

Figure 16. Deformation vs time (300 mm long).

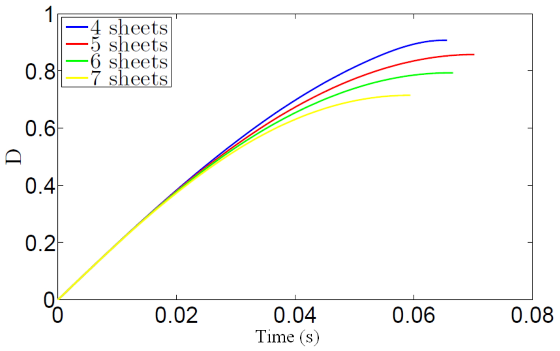

Figure 17. Deformation vs time (350 mm long).

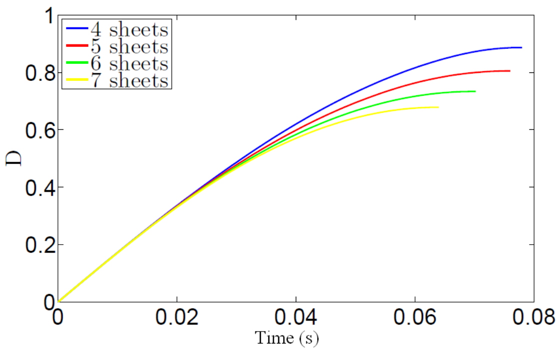

Figure 18. Deformation vs time (400 mm long).

A 300 mm long with 6 sheets attenuator (Figure 19, 20) appeared to be able to guarantee good performances with minimum weight, about 3 kg. In Figure 21 is represented the attenuator deformation sequence during the impact phenomenon.

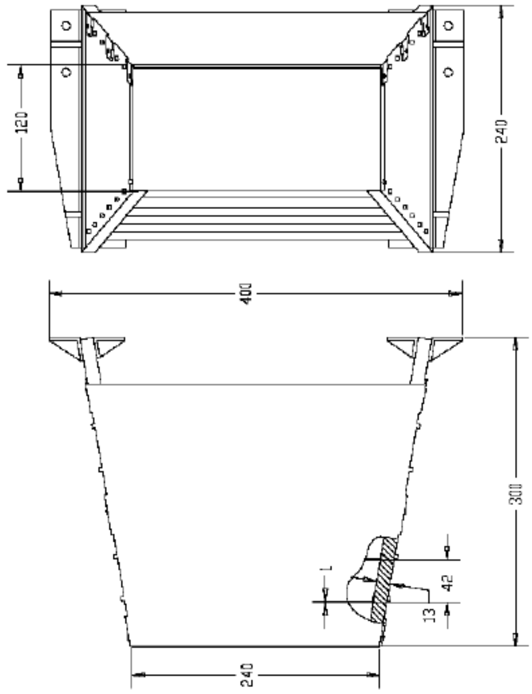

Figure 19. Draft of the attenuator.

Figure 20. Real crash-box.

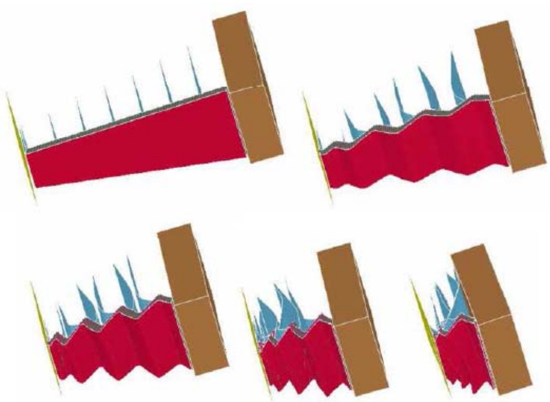

Figure 21. Frames of simulation.

CONCLUSIONS

The present paper describes a numerical investigation of an energy absorber for a Formula SAE race car. A finite element model has been developed using LS-DYNA code doing a simplified optimization process in order to obtain the best configuration of crash-box in terms of average deceleration and stroke efficiency. On the test and numerical results the proposed procedure appeared to be adequate to design the attenuator from the practical application point of view of the considered sport car.

REFERENCES

[1] LS-DYNA, Keyword User's Manual, Version 971, LSTC, 2006;

[2] E.Wu, W.-S.Jiang, "Axial Crush of Metallic Honeycombs", International Journal of Impact Engineering, Vol. 19, 439-456, 1997;

[3] S.-T.Hong, J,Pan, T.Tyan, P.Prasad, "Dynamic crush behaviours of aluminium honeycomb under compression dominant inclined loads", International Journal of Plasticity, Vol.24, 89-117, 2008;

[4] H.Zhao, G.Gary, "Crushing behaviour of aluminium honeycomb under impact loading", International Journal of Impact Engineering, Vol.21,827-836,1998;

[5] L.Aktay, A.-F.Jhonson, M.Holzapfel, "Prediction of impact damage on sandwich composite panels", Computational Material Science, Vol.32, 252-260, 2005.